Multifractal fracture-toughness properties of brittle heterogeneous materials

1996 J. Phys. A: Math. Gen. 29 2657

(http://iopscience.iop.org/0305-4470/29/11/007)

J. Phys. A: Math. Gen. **29** (1996) 2657–2670. Printed in the UK

Multifractal fracture-toughness properties of brittle heterogeneous materials

Mark J Meisner and George N Frantziskonis

Department of Civil Engineering and Engineering Mechanics, University of Arizona, Tucson, AZ 85721, USA

Received 20 July 1995

Abstract. This paper documents a study of novel fracture-toughness properties of brittle heterogeneous materials. Through simulations of the rupture process based on a lattice discretization of the material, the spatial variation of dissipated energy due to fracture is evaluated. Under certain conditions, its distribution is characterized by a multifractal spectrum $f(\alpha)$. Importantly, $f(\alpha)$ depends not only on the initial heterogeneity present in the material but also on the nature of the externally applied load. This provides a renewed load-path-dependent definition of fracture toughness material properties. It avoids the difficulties associated with 'traditional' continuum/fracture mechanics definitions where the macroscopic fracture mode must be known *a priori*.

1. Introduction

Materials of technological/scientific interest are infrequently perfectly homogeneous. In many cases the existence of spatial disorder is highly desirable, as in, for example, concretes, rocks, ceramics, composites and other brittle heterogeneous materials. Disorder may be due to the presence of different constituents such as aggregates, pores, micro-cracks and interfaces. In other words, localized spatial variations in material properties are directly attributed to the material microstructure. An inhomogeneous microstructure will have a significant effect on the fracture behaviour of brittle materials, a subject of substantial technological importance.

The main focus of the present study is on toughness, i.e. the energy dissipated during the process of rupture, and the properties of brittle heterogeneous materials under various external loading conditions. A fundamental notion used herein is that fracture of the material is dependent upon the spatially varying material properties present before the external loading process begins. In particular, the actual spatial disorders of the initial local elastic and failure values are reduced to either spatially correlated or uncorrelated random 'fields'. As discussed in further detail later, information on the (statistical) properties of such fields can be obtained experimentally via non-destructive evaluation methods [1], or provisionally [2, 3], or on a purely geometrical basis [4]. As a result, knowing the (statistical) spatial disorders of the material allows the use of a statistical mechanics approach to simplify and solve inhomogeneous structures, i.e. specimens, subjected to intense external loading conditions.

Using a statistical mechanics strategy, it is readily possible to capture some of the essential rupture-related behaviours of a brittle material. The fractured structures contain irregular crack networks in which information about the material may be obtained.

0305-4470/96/112657+14$19.50

Consequently, once the cracks have been characterized, important phenomena may be quantified, such as material resistance to crack formation and dissipated energy due to fracture. Characterization of the crack networks may become possible through the use of sets of scaling exponents. As a result, in such cases, scaling laws may be implemented [5]. In short, scaling laws are examined herein in order to quantify several of the resulting properties of the fracture process.

The present study was inspired by the work of Herrmann *et al* [6] and Hansen *et al* [7] where a two-dimensional beam and central force lattices were utilized, respectively, within the context of statistical mechanics, to study rupture of disordered media. In these studies a quenched spatially uncorrelated disorder in the breaking thresholds of the beams and bars, respectively, was considered. For both lattice configurations the distribution of local forces just before the final completion of the rupture process was found to be multifractal. At that instant, the moments (M_n) of order n of the local forces F can be characterized by a scaling exponent $y(n)$, i.e. $M_n \propto L^{y(n)}$ where L is the size of the lattice. Then it is straightforward to show that the energy stored in the system, proportional to F^2 since the system is linear and elastic, is multifractal. This then implies that the complementary energy, the energy dissipated in the process of fracture, should be multifractal. The dissipated energy is a measure on the fracture network, and this provides further physical interpretation of the multifractal properties—provided the underlying fracture network is fractal, the dissipated energy (measure) on it could possibly be multifractal [5]. Since this energy is characteristic of the material fracture toughness, it is interesting to study the distribution of dissipated energy. Frantziskonis [8, 9] studied this problem analytically (in two dimensions)—solutions became possible for a certain limit and specialized cases discussed subsequently. The analytical solutions suggest that the dissipated energy can indeed be multifractal. In particular, the so-called p-model multifractal was investigated. Since analytical solutions have only been obtained for certain cases of rather limited generality, in this study more general numerical results are presented.

For simplicity, the fracture process of brittle heterogeneous materials will be investigated through the use of the two-dimensional central force lattice model. In section 2, a discussion of the lattice framework model with respect to the present study is presented. This is necessary since 'traditional' fracture-toughness properties are defined within the context of elasticity (or continuum mechanics in a more general framework); thus a 'connection' to the present study should be established. In section 3, the concept of a fractal is applied to find fracture surface/network related parameters; finally, the multifractal nature of the dissipated energy is illustrated in section 4.

2. The numerical model

Analytical solutions to the differential equations of the elasticity theory are often impractical or impossible to obtain due to mathematical difficulties. There are several methods to obtain numerical solutions, a review of which is beyond the scope of this paper. Fracture toughness is principally defined within the context of continuum elasticity theory. In the following the lattice-based numerical analysis used herein is discussed with respect to classical elasticity theory. This is so that the continuum mechanics based definitions and available results on toughness are 'compared' to the present study. Further, the continuum mechanics based analytical solutions presented in [8, 9] can be compared with the results of the present numerical study.

An appropriate lattice discretization, i.e. replacing the body of a material with a framework of bars (elements), is a consistent method for the solution of elasticity problems—

cf Hrennikoff [10] as well as recent publications referred to below. Arrangement of the bars is performed according to a specific pattern, in which individual elements are assigned particular elastic and fracture properties. In addition, boundary and internal stresses and corresponding displacements of the model are distributed over the tributary bars in order to obtain the equivalent stresses and displacements of the original elastic body. In other words, the lattice is formed by using the same geometric outline, boundary conditions and loads of the original solid body (which may even contain micro-cracks). External loads, either given displacement or traction, are applied at the nodes (joints). Consequently, with a few qualifications which will be discussed next, the lattice method may be applied to an immense variety of situations and allow convenient and accurate modelling of the original (continuum) structure.

A necessary and sufficient condition for the equivalent mechanical behaviour of the lattice model and the original solid material is equality of the deformation, simply because deformability is the one physical characteristic which will determine the stresses throughout the media. This has been demonstrated [10], i.e. when the element size of the lattice (the spacing) is small enough compared to the length scale above which information is sought. Accordingly, a lattice of small finite-sized elements will give a framework which closely resembles the original mechanical system. Although it is not exact, the lattice method yields solutions to a number of problems in which formal implementation of the elasticity theory fails. For highly heterogeneous materials, the lattice spacing is crucial in representing the material microstructure. This is discussed further below.

Triangular two-dimensional framework systems are considered herein. The bars may either articulate about the nodes (rotate freely) or be devoid of any rotational behaviour. The former case is presented and used in this study. This framework is known as the central-force lattice model. It is noted that for the type of framework chosen the conditions of deformability may be satisfied for only one value of Poisson's ratio, which is $\frac{1}{3}$—this is applicable for any isosceles triangular central-force lattice system. If other values of Poisson's ratio are desired, other framework patterns must be considered. However, for the present study the developed value of $\frac{1}{3}$ will suffice.

The spatially dependent material properties are fixed before the loading (rupture) program begins. This is known as a quenched disorder process. Some of the local material characteristics which may be implemented into the lattice model are density, elastic modulus and failure strength. It has been shown through non-destructive experimental evaluation [1] that some heterogeneous brittle materials have a quasi-constant local density to local elastic modulus ratio. It is concluded that for length scales larger than a typical scale (i.e. the grain size in a granular or polycrystalline material) it is, rather, the failure strength that varies spatially in a fashion important for fracture. Although further research in this important area is necessary—cf [1] for an extensive discussion—based on current knowledge and in order to reduce the number of possible material parameters, this condition will be assumed for the present case. As a result, the characteristics of the modelled engineered material will be reflected in the failure strengths of the individual elements.

Each element is endowed with its own particular value of failure strength, S. Under the assumption that the elements are ideally linearly elastic and brittle, a bar will break when the force to which it is subjected exceeds S (for compression) or T (for tension). The relation between the absolute values of the compression and tension breaking parameters is given by $T = RS$, where R may be defined for each element. However, for simplicity, only the case of symmetric rupture criterion is considered ($R = 1$). For simulation purposes, S is considered, in general, to be a random field. The choice to consider spatial correlations in S (a special case calls for S being a spatially uncorrelated random variable) was based

upon many factors:

- the lattice spacing is assigned to be equal to the lower 'cut-off' of material heterogeneity, a scale characteristic of the microstructure, in general much larger than the atomic, i.e. the grain size in a granular material. The presence of heterogeneities at larger scales, i.e. larger aggregates in a concrete material, introduce spatial correlations.
- even in the absence of heterogeneities at larger scales, the geometrical arrangement of the constituents naturally introduces spatial correlations, i.e. consider a packing of (equal size) spheres as a two-phase material and the spatial correlations on either of the two phases.
- it is feasible to determine the statistical properties of actual heterogeneous materials experimentally, i.e. as done by Breysse *et al* [4], or as suggested by Dai and Frantziskonis [1]. For example, it has been found that for a typical concrete material, a spatial material properties correlation length appears to be equal to a few times the maximum aggregate size or a few times the average distance between the large aggregates.

Despite the presence of very encouraging results in the literature, further research is needed to identify the statistical properties of actual materials precisely. Lack of complete information at this time should not, however, discourage investigations along the lines suggested herein. Thus, in the following, S is considered to be statistically stationary with a Gaussian autocorrelation function. Its expected value, variance, and (auto-) correlation length provide, then, complete statistical information on S. The correlation length of S, ℓ_S, is the radius of a circle beyond which S ceases to be correlated [11].

This approach to solid mechanics problem solving allows a natural induction of disorder into the model and a physical interpretation of the algorithm is readily available. In other words, use of the lattice numerical model in conjunction with spatially correlated material properties suggests a 'connection' between a purely statistical mechanics approach to fracture, i.e. [7], and a continuum/fracture mechanics approach which is based on homogenized values of material properties and crack propagation through a mathematically homogeneous solid. For infinitely long correlations the problem reduces to a 'continuum/fracture mechanics' one, while the spatially uncorrelated problem is a 'pure statistical mechanics' one. Once the continuous elastic equations have been discretized into a set of coupled linear equations, with the imposed boundary conditions, the system of equations may be solved by an efficient algorithm. If the boundary conditions consist of displacement constraints, then the coupled equations are directly modified; this is performed explicitly in the equations which correspond to the constrained nodes. A variety of externally imposed displacement loading conditions are investigated: uniaxial tension, dilatation and shear. Hence, with the boundary conditions implemented accordingly, the set of equations are solved by a defined algorithm, which will be described next.

The simulation of the displacement loading process on the lattice is done in an iterative manner. First, the system of equations is solved in order to determine which elements may be broken under the current load. After an element is broken, the system must be solved again to find the updated stress field in order to break the next bar, and so on. Inertia forces are ignored and crack propagation is considered to be 'slow', i.e. there is enough 'relaxation time' before further rupture occurs. Note that crack propagation can be dynamic even if the external load is applied slowly—cf [9] for discussion; however, this case is not considered in this initial study. That is to say, the simulation algorithm used for the model consists of:

(i) calculating the stress and displacement field of the system of equations;

(ii) determining which elements are eligible to be broken (according to individual lattice elements fracture criteria);

(iii) removing (breaking) the element that has the highest absolute values of the ratio of stress and S;

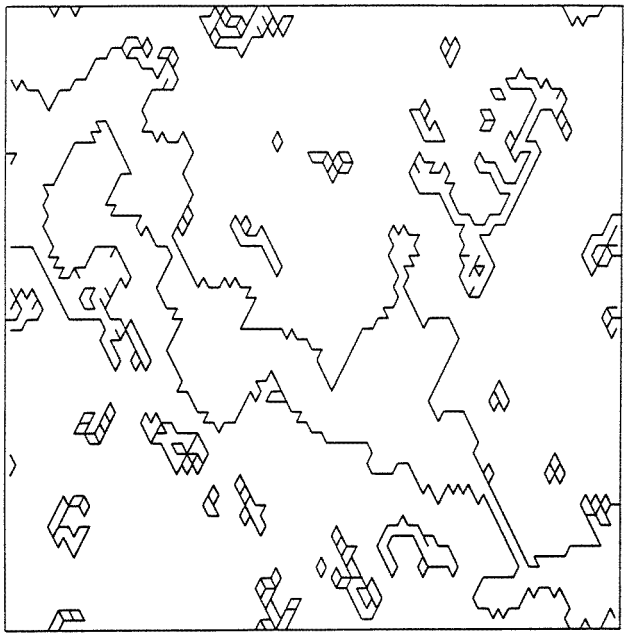

Figure 1. Example of the rupture process. The external load is applied in uniaxial tension mode in the vertical direction. The lines show the crack surfaces. One major through-the-width crack network, responsible for final failure, can be identified.

(iv) resolving the system;

(v) repeating steps (ii) through (iv) until the system reaches complete fracture.

For a typical example of the rupture process for uniaxial tension displacement boundary conditions in the vertical direction, which is illustrated by the developed crack surfaces, see figure 1.

3. Fracture network properties

The concept of scaling has proven to be quite valuable in quantifying some of the properties of heterogeneous materials, thus the literature relevant to scaling properties of fracture networks/surfaces is very rich. Several experimental, numerical and theoretical studies have been reported, and for a recent review and trace of the literature we refer to Roux [12]. Despite the large number of publications on the subject, several issues are not well understood. For example, there is not, to our knowledge, a concrete physical explanation for the observed (experimentally) or calculated (numerically) fracture surface scaling properties. From this perspective, investigation of the associated dissipated energy as suggested herein is expected to provide further insight.

The fracture surface/network properties are defined through scaling exponents. In certain cases, there is a correlation between these exponents and toughness: as shown herein, a positive correlation. Let us first review briefly the process of study followed herein, which is that of Matsushita and Ouchi [13], and then discuss how it is 'adapted' for particular cases. Suppose that a curve (i.e. a fracture network) is represented, in two-dimensional space, by $y = f(x)$. Let a (=1), be of unit length, defined as the smallest length scale of the curve. On the curve, two arbitrary points, A and B, are chosen. The distance between

A and B along the curve is measured and given in terms of Na $(=N)$. Next, the x- and y-variances, var(x) and var(y), respectively, are calculated from measured points on the curve between A and B. These variances are defined as

$$\text{var}(x) = \frac{1}{N-1}\sum_{i=1}^{N}(x_i - \mu_x)^2 \tag{3.1}$$

$$\text{var}(y) = \frac{1}{N-1}\sum_{i=1}^{N}(y_i - \mu_y)^2 \tag{3.2}$$

where

$$\mu_x = \frac{1}{N}\sum_{i=1}^{N} x_i \tag{3.3}$$

$$\mu_y = \frac{1}{N}\sum_{i=1}^{N} y_i \tag{3.4}$$

and (x_i, y_i) is the coordinate of the ith measured point on the curve. This procedure is repeated for many sets of points A and B on the curve. Finally, log–log plots of the x and y standard deviations versus N are used to see if they scale as

$$x \sim N^{\nu_x} \qquad \text{and} \qquad y \sim N^{\nu_y}. \tag{3.5}$$

As is clear from [13] the ratio ν_y/ν_x can be used to characterize a self-affine curve if its substrate is known or can be calculated. For self-similar curves, $\nu_y = \nu_x$, thus measures other than ν_y/ν_x i.e. the inverse of ν_y or ν_x could/should be used in this case, which implies that $\nu_y = \nu_x$. As explained in the following, a substrate is not clearly identifiable for the problems we studied. Thus, although ν_y and ν_x are direction dependent, in the case where a substrate is not identifiable/present they (actually their inverse) can be seen as anisotropic correlation lengths. (As mentioned by Matsushita and Ouchi [13] such lengths are used in critical phenomena such as in liquid crystals.) For example, if we consider the (very anisotropic) case of a straight line, when its direction is not specified, i.e. when each direction between 0° and 360° has equal probability of being realized, then one would get $1/\nu_y = 1/\nu_x = 2$ (i.e. a space filling 'curve') which implies equal probability of direction. Thus for our case the reason why a substrate is not identifiable/present needs to be explained, and this is explained in the following paragraph.

Let us consider the uniaxial tension problem, where load is applied in the y direction. In the fracture problem studied along the lines of [14] since the initial crack starts in the middle of the specimen and since fracture is 'controlled' to propagate along a specifically defined 'neighbourhood', the final crack ends up being more or less parallel to the x direction, i.e. the substrate is identifiable in this case. Although this may have a clear physical interpretation, i.e. for certain materials, for our problem, the crack(s) initiate at the location(s) dictated by the problem. Due to interactions with the free as well as with the loaded surfaces, it may be shown [15, 16] that cracks are most likely to initiate near the boundaries; however, although such 'surface effects' are important, the following conclusions also hold, in general, independent of boundary effects, i.e. for an infinite 'specimen'. In the problem studied in our work, fracture initiates, in general, either concurrently or sequentially, at more than one (i.e. at several) regions. Subsequently, a few small fracture 'clusters' are formed, and final fracture (separation of the specimen into two or more parts) occurs by coalescence of a few such clusters, usually two but often three or more. In passing it is noted that occasionally (for some realizations), especially when the ratio of material correlation length

Table 1. Calculated values, $L = 40$ (40×40 lattice), $\ell_S/L = 1.0$.

	Uniaxial Tension		Dilation		Shear	
COV	$1/\nu_x$	$1/\nu_y$	$1/\nu_x$	$1/\nu_y$	$1/\nu_x$	$1/\nu_y$
0.1	1.15	1.27	1.31	1.32	1.65	1.63
0.2	1.20	1.33	1.36	1.35	1.75	1.71
0.3	1.27	1.36	1.37	1.38	1.75	1.72
0.4	1.27	1.38	1.42	1.43	1.78	1.79
0.5	1.30	1.38	1.48	1.46	1.85	1.83

over specimen length is large (i.e. close to unity) a single crack forms. Thus, in general, a substrate cannot be defined, since for each realization of the problem such a substrate is formed randomly. Thus, it is made clear that $1/\nu_y$ and $1/\nu_x$ should be interpreted in the form of anisotropic correlations rather than as fractal dimensions. Finally, it is mentioned that even a case which calls for $\nu_y = \nu_x$ does not exclude the possibility that each (or some) realizations of the problem show a self-affine fracture 'surface'. Locally, of course, i.e. in regions where a substrate is assigned/assumed, a self-affine surface may always be present.

Simulations of the fracture process are performed and ensemble averages of the quantities of interest are calculated. Here only typical results are presented; a complete report of the results can be found in [17]. Without loss of generality, the mean of S has been defined to be unity. As a typical correlated case and/or material structure (specimen) of the order of the correlation length, the ratio $\ell_S/L = 1.0$ was considered. This ratio is approximately the one for real samples, i.e. for concrete (correlation distance and sample size are both of the order of a centimetre), large grain size ceramics (of the order of a millimetre). The values of ν_y and ν_x were calculated for three displacement loading cases—uniaxial tension, dilatation, and shear. The results of these simulations are given in table 1.

This table was developed from 50 numerical realizations of 40×40 lattice size (a larger number of realizations changed the values shown above slightly and rather insignificantly). Three trends can be identified from the data, for varying fluctuations of the random fields, i.e. coefficient of variation, COV $= 0.1$, 0.2, 0.3, 0.4, and 0.5. First, anisotropic (global) correlation seems to be the case for uniaxial tension while isotropic correlation holds for dilatation and shear loading. This could be directly due to the symmetric loading placed on the framework in this case. The second observation is that both $1/\nu_x$ and $1/\nu_y$ tend to increase in the order of uniaxial tension, dilatation, and shear loading. As a result, it may be concluded that the triangular lattice has 'toughness' which is dependent on the loading environment; this will be examined in the next section. Last, as the fluctuations increase (for increasing COV) $1/\nu_x$ and $1/\nu_y$ increase slightly, due to the 'tortuosity' of S and related stress concentrations. As a result, it may be that as the fluctuations increase the material toughness increases as well. For the influence of correlations, as ℓ_S/L increases $1/\nu_x$ and $1/\nu_y$ decrease and for a large enough ratio (homogeneous case) $1/\nu_x$ and $1/\nu_y$ tend towards unity (straight crack pattern). As ℓ_S/L decreases, $1/\nu_x$ and $1/\nu_y$ increase slightly. In the following, the dissipated energy, the central theme of this work, is examined.

4. Multifractal properties of the dissipated energy

There are many physical quantities where in order to have an exhaustive characterization of their distribution, the implementation of an infinite series of scaling exponents may be

necessary. Such generalized quantities can be equivalently described by the corresponding multifractal spectrum, i.e. [18]. In other words, a description of a distribution (measure) that is multifractal in nature may be described by the corresponding $f(\alpha)$ versus α curve. Thus, the infinite set of scaling exponents are characterized by their singularities and the Lipshitz–Hölder exponent, α, determines the strength of the singularities. Consequently, a multifractal measure consists of interwoven sets of singularities which are characterized by their dimension that is given by $f(\alpha)$.

The case in which the crack dissipated energy of a brittle heterogeneous material is multifractal in nature is examined. Instead of the 'strictly' continuum case examined analytically [8, 9], the dissipated energy is quantified by employing the central-force lattice model. Accordingly, the multifractal spectrum must be defined in terms associated with the lattice model in a rather 'standard' fashion, i.e. as presented in [19].

For future reference, a moment of order n of the crack dissipated energy is defined by

$$\langle E^n \rangle = \sum_{i=1}^{\text{all bins}} |E_i|^n N_i(E, L) \tag{4.1}$$

where $N_i(E, L)$ is the histogram of the dissipated energy rescaled with respect to $\max(|E_i|)$ and the sum is over all the bins of the histogram.

As mentioned above, it is possible to describe the crack dissipated energy in terms of an infinite set of scaling exponents or by its Legendre transformation (the $f(\alpha)$ spectrum). Accordingly [19], the study is made by plotting $\log(N_i(E, L)/\log(L)$ versus $\log(E)/\log(L)$, the rescaled log-histogram of the dissipated energy distribution. As a result, if the distribution is not multifractal, only a single point will be obtained; otherwise, the resulting curve will tend to be size-independent for large lattice sizes. It is made clear that the distribution of energy (energy released by each element that has been broken) at the final stage of rupture is examined, i.e. at the same point where the multifractal properties of the load distribution are studied in, for example, [7]. Further, it is noted that for the case of extreme disorder, i.e. when $\ell/L \to 0$ and the COV of the failure threshold is extreme, would be at percolation threshold and the dissipation energy will be multifractal [20]. For other cases, i.e. for the ones studied in our work, where ℓ/L has a non-zero value and the disorder is not extreme, at rupture (where the dissipated energy is studied) we have a sort of 'specialized' percolation case, in the sense that a connection of broken bars from one side of the specimen to the other is formed. It will be interesting to study the distribution of dissipated energy before final fracture or the one recorded during the process of progressive fracture, i.e. as done for problems relevant to 'classical' (not specialized) percolation by Roux and Hansen [20].

If it is assumed that the moments are self-averaging, then $E^n N_i(E, L)$ will peak somewhere in the sum; using this assumption and the saddle point method, i.e. [21], equation (4.1) may be written as

$$\langle E^n \rangle \approx \int_0^1 E^n N_i(E, L)\, \mathrm{d}E \approx L^{y(n)}\,. \tag{4.2}$$

For completeness, and in order to be as self-contained as possible, the interpretation $f(\alpha)$–α, the formalism for the moment equivalence for a multifractal is given. The integral in (4.2) may be rewritten using a change of variable,

$$\alpha(E, L) = -\frac{\log(E)}{\log(L)} \tag{4.3}$$

as

$$\langle E^n \rangle \approx \int_0^1 L^{-n\alpha(E,L)+f(E,L)}\,\mathrm{d}E \tag{4.4}$$

where

$$f(E,L) = \frac{\log(N_i(E,L))}{\log(L)}\,. \tag{4.5}$$

In addition, another consequence of the self-averaging assumption is that the peak will be pronounced for a particular value of E. The position of the peak, which will lead to the relation between scaling exponent $y(n)$ and the multifractal spectrum, is determined by taking the derivative of the exponent in (4.4),

$$\left.\frac{\partial f(\alpha,L)}{\partial\alpha}\right|_{\alpha=\alpha(n)} = n\,. \tag{4.6}$$

The moment of the crack dissipated energy is then approximated by using (4.4) and (4.6), giving

$$\langle E^n \rangle \approx \int_0^1 L^{-n\alpha+f(E,L)}\,\mathrm{d}E \tag{4.7}$$

$$\approx L^{-n\alpha(n)+f(\alpha(n),n)} \tag{4.8}$$

$$\approx L^{y(n)} \tag{4.9}$$

where

$$y(n) = -n\alpha(n) + f(\alpha(n),L)\,. \tag{4.10}$$

Since $y(n)$ is independent of L, it follows that

$$f(\alpha(n),L) = f(\alpha(n)) = f(\alpha)\,. \tag{4.11}$$

All in all, the Legendre transformation of $f(\alpha)$ and α to $y(n)$ and n, respectively, has been developed.

The method of examining the possible multifractal properties of dissipated energy is similar to that reported in [7, 6]. Figure 2 shows a typical rescaled log-histogram of the dissipated energy distribution at the failure state for different lattice sizes. A good collapse of the data, especially with increasing lattice size, is observed. It is noted that the number of simulations employed decreased with increasing lattice size. The numerical data associated with the highest of energies are not shown in this and in subsequent figures, due to finite size effects. In other words, the collapse of the data for high energies (small α) is unacceptable. There are two possible reasons for this. First, the number of broken elements with very high energies is small compared to the total number of broken bars, and hence, a good statistical sample is not obtained. Second, localized clusters of high energy regions may be too large compared to the lattice size for appropriate stochastic analysis.

In figure 2 as well as in figure 3 a thin full curve corresponds to the p-model $f(\alpha)$ curve and it is discussed subsequently. Figure 3 shows typical results for uniaxial tension, dilatation and shear. Although the lattices considered are rather small to make any definite conclusions, the fact that these plots tend to be size-independent (for increasing lattice size, although the 'collapse' is not shown here for clarity in the figures) provides evidence that the dissipated energy distribution is multifractal. It is noted that the log-histogram collapsed into a single point (which implies a homogeneous fractal) for the zero disorder cases, where COV $= 0$.

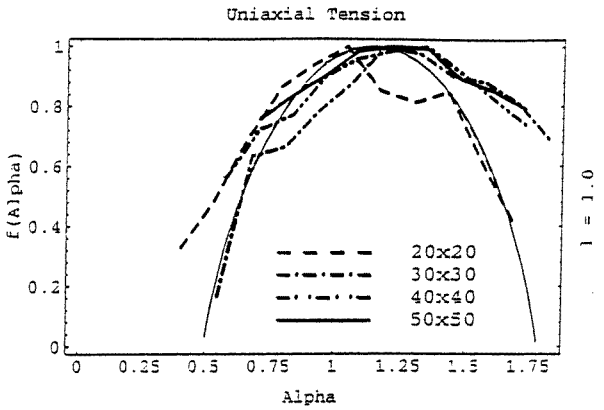

Figure 2. Rescaled log-histogram of the dissipated energy obtained from four different lattices ($L = 20$, 30, 40, 50) subjected to uniaxial tension. The coefficient of variation of S is 0.2 and $\ell_S/L = 1$. The thin full curve corresponds to the so-called p-model multifractal, and is discussed further in this paper.

An analytical solution to the problem of the crack dissipated energy would be useful for comparison with the numerical approach of the lattice formalism, as well as the understanding of brittle fracture. Under certain conditions there is a strong possibility that the dissipated energy distribution is multifractal [8, 9]. The proposed model is the (commonly used) so-called p-model [22]. Using the notation of [9, 22], the generalized dimensions are given by

$$D_q = \{p_1^q + (1 - p_1)^q\}^{1/(1-q)} \tag{4.12}$$

where p_1 designates normalized dissipated energy along a (straight) crack of length equal to the lower cut-off considered in the analysis. A value of $p_1 = 0.5$ indicates a homogeneous fractal, while the lower its value the higher the spatial disorder in the dissipated energy. Given the value of p_1, the expression for the multifractal spectrum is given in terms of a dimensionless parameter ζ,

$$\alpha = \frac{\log_2(p_1 + 1) + \log_2(1 - p_1)}{\zeta} \tag{4.13}$$

and

$$f(\alpha) = \frac{\zeta \log_2(\zeta)(\zeta - 1)\log_2(\zeta - 1)}{\zeta}\,. \tag{4.14}$$

Parameter ζ may be eliminated, giving the explicit expression for $f(\alpha)$ as a function of α, with only one parameter, p_1. Under certain conditions it was possible to find the value of p_1 analytically [9]. The analytical solutions are approximate and were obtained under several simplifying assumptions:

- crack propagation was considered 'fast', i.e. singularities in front of a running crack tip were ignored. Physically, this assumption implies that the crack is running at a velocity high enough for the stresses to redistribute between two successive crack extensions of small (equal to the lower cut-off) length.
- the material was considered incompressible, and this allows introduction of a stream function and simplifies representation of the strain field. This implies a Poisson's ratio equal to 0.5.

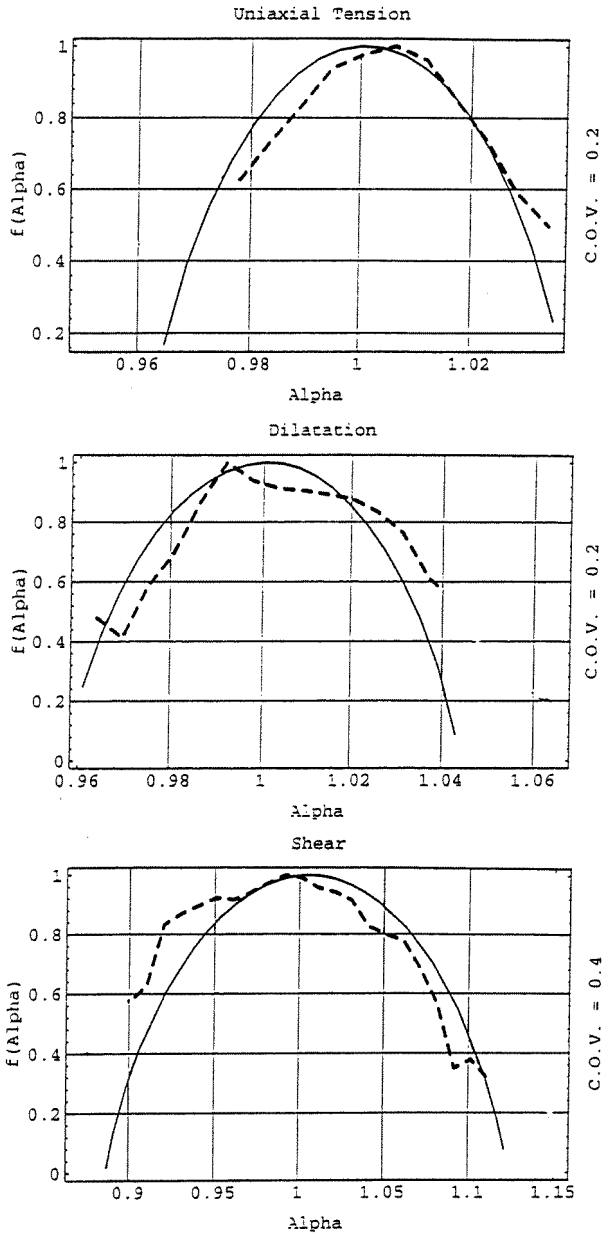

Figure 3. Typical rescaled log-histogram (broken curve) of the dissipated energy obtained from $L = 40$ lattices (*a*) uniaxial tension, (*b*) dilatation, (*c*) pure shear. For all three cases, $\ell_S/L = 1$, and the full curve corresponds to the *p*-model multifractal discussed subsequently. For cases (*a*) and (*b*) COV $(S) = 0.2$, while for case (*c*) COV $(S) = 0.4$.

• it was not possible to obtain an analytical solution for the case where the failure threshold S is a random field. Instead, the micro-strains were considered to be spatially correlated random fields. The implications of this assumption are examined later.

• the analytical solution presumes that fluctuations are small, so that a relevant Taylor series expansion is valid.

It seems, at first glance, that the analytical solutions are for cases different to the ones the numerical results were obtained. Although it is difficult to 'produce' numerically stationary random micro-strain fields in the sense examined analytically [9], it is crucial to note that the rupture problem examined is incrementally linear—between successive bond breaking a linear problem is solved. Then, consider a crack tip (far from boundaries and/or other cracks) and the instant before it extends by a small distance, that distance being equal to the lattice spacing or the lower cut-off for the analytical (continuum) case. In the case where the only disorder is in S (like the numerical results) the stress field in front of the crack is that predicted by theory of elasticity (with a homogeneous material), i.e. the stress is proportional to $kr^{-\lambda}$, r being the distance from the crack tip, k being the stress intensity factor, and $\lambda = 0.5$ for the classical fracture problem. Thus the crack-extension direction is merely the weak direction in front of the crack and this is dictated by the S-field. The magnitude of the dissipated energy during this crack extension is also governed by the S-field, i.e. by the value of the failure stress in the weakest direction in front of the crack tip. In the case where the only disorder is in the strain field (like the analytical solution) since singularities were ignored (assumption 1) the crack-extension direction is again governed by the weak direction in front of the crack and this is in turn dictated by the strain field. The magnitude of the dissipated energy during this crack extension is again governed by the strain field. Thus, if the statistical properties of S for the numerical case and that of the strain field for the analytical case are similar, the statistical properties of the dissipated energy for the two cases should be similar. One major difference results from the fact that as the size of the lattice increases, the stress intensity factor changes, and thus the α singularities may be slightly different in the numerical solution case (S being random) to that in the analytical one. Thus, the α value for the analytical solution (horizontal axis in figure 3) was replaced by $\alpha - c$, c being a constant such that the peak values of the $f(\alpha)$ curves collapsed. The above, then, explains the 'good' comparison between the analytical and numerical solutions shown in figure 3. The following important points should be mentioned.

Figure 4 shows the analytically predicted values of p_1 as a function of COV, for a relatively spatially uncorrelated case, (a) where $\ell_S/L = 1/30$ was considered for the micro-strain field, and (b) for a strongly correlated case ($\ell_S/L = 1$). Figure 4(a) suggests that the disorder in the dissipated energy pattern is highest for the pure shear case, followed by the tension and dilatation cases. However, figure 4(b) suggests that the 'order' between tension and dilatation is opposite. It is interesting that numerical results first suggested such differences between uncorrelated and strongly correlated cases, which was then backed up by the analytical solution readily available.

Experimentally, it is known that fracture toughness as measured from a shear experiment is higher than that measured from a tension test (dilatation tests are seldom performed). This agrees with the curves shown in figure 4, where for constant specimen size, the lower value of p_1 will result in increased energy dissipation. Additionally, if we consider that ℓ_S is characteristic of the material, then the curves in figure 4(a) would correspond to a structure (specimen) 30 times larger than that in figure 4(b). It could be 'instructional' to evaluate normalized (per material volume) dissipated energy for both such cases. However, the problem of 'similitude' in fracture-related parameters is a rather complicated subject where effects like rate of loading, plasticity, relative values of yield stress and elasticity modulus come into picture. This exact subject is currently being examined in the context of the results presented here.

In closing, we discuss some points relevant to the use of $f(\alpha)$ as a measure of toughness. Given the evidence of multifractal distribution of dissipated energy, the total energy dissipated in a specimen will be strongly dependent on its underlying distribution which,

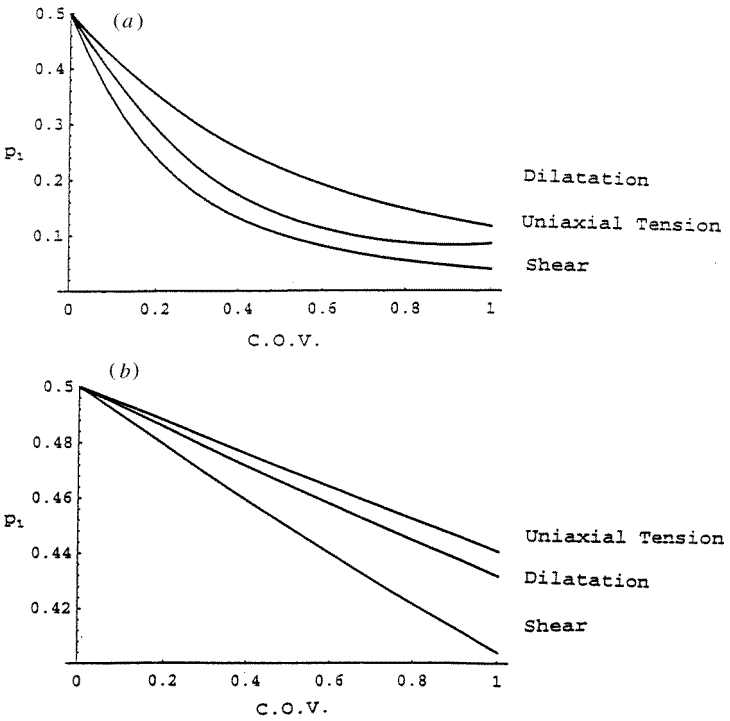

Figure 4. Analytical values of p_1 as a function of COV (a) for a relatively spatially uncorrelated case, $\ell_S/L = 1/30$, (b) for a strongly correlated case, $\ell_S/L = 1$.

in turn, is related to the initial heterogeneity of the material. Thus, the present approach shows promise in establishing a fundamental relationship between material microstructure and toughness. As another implication, toughness is shown to be size/shape-dependent as well as dependent on the external loading conditions. Another aspect where the properties of the dissipated energy distribution are of use is in identifying what parts, i.e. the 'strong' or the 'weak' ones in a gross sense, of a material are the major toughness contributors. Experience, cf discussion in [1], has provided evidence that, depending on the specific spatial disorder present, some materials dissipate energy mainly in their 'strong' regions, while others in their 'weak' ones. We believe that work along the lines of the present paper provides a fundamental framework for studying such important tasks closely. Of course, the present work is amenable to several possible experimental verifications. A combination of non-destructive, destructive and numerical work seems to be promising. Several possibilities for extension and/or verification of the present work exist, an example is given in the following. Non-destructive evaluation techniques can identify the initial spatial distribution of material properties. Then, a combination of (experimental) investigation of the fracture network/surfaces and numerical analysis of the problem of the distribution of dissipated energy can provide the relevant $f(\alpha)$. This should provide a relation among initial material heterogeneity, properties of the fracture surfaces/network, and energy dissipated for its development. By comparing with the total energy dissipated in a sample (measured experimentally) and by studying the cracks not interconnected with the main one(s), information on the so-called fracture process 'zone' can be obtained. This is partly the reason why cracks not connected with the main one(s) were not included in the present analysis (dissipated energy distribution). It seems that for some materials such a process

zone is important while for other ones it is negligible, and this needs to be investigated on a fundamental basis.

5. Conclusions

Through a lattice-based numerical approach, renewed fracture-toughness related parameters are suggested. In particular, the $f(\alpha)$ curve of the dissipated energy shows considerable promise in serving as a material-, structure-, as well as load-path-dependent set of characterization parameters. Thus, it is suggested herein that fracture toughness should not be defined independently of the nature of the external load applied to a structure or even independently of its geometry (size, shape). Further, the p-model, when applicable, provides an even further simplified description in terms of one number, namely p_1. In passing, an important connection between a purely statistical mechanics and a continuum-based approach to the problem of rupture and toughness is addressed. Finally, it is stressed that this work is amenable to experimental and further numerical verifications—some paths towards this are discussed.

Acknowledgments

The present research was supported partially by a grant from the University of Arizona Foundation to MJM, and by grants from the National Science Foundation, Washington DC, Grant no MSS/PYI/9157237, and the Hughes Aircraft Company to GNF. Two-dimensional random fields were created by the spectral representation method [23]. It is a pleasant duty to thank the authors for providing the relevant code.

References

[1] Dai H and Frantziskonis G 1994 *Mech. Mater.* **18** 103
[2] Schlangen E and Van Mier J G M 1992 *Mater. Struct.* **25** 534
[3] Murat M M, Anholt M and Wagner H D 1992 *J. Mater. Res.* **7** 3120
[4] Breysse D, Fokwa D and Drahy F 1994 *Appl. Mech. Rev.* **47** (p2) S184
[5] Mandelbrot B B 1983 *The Fractal Geometry of Nature* (San Francisco: Freeman)
[6] Herrmann H J, Hansen A and Roux S 1989 *Phys. Rev.* B **39** 637
[7] Hansen A, Roux S and Herrmann H J 1989 *J. Physique* **50** 733
[8] Frantziskonis G 1994 *Eur. J. Mech. A/Solids* **13** 73
[9] Frantziskonis G 1994 *Appl. Mech. Rev.* **47** p2 S132
[10] Hrennikoff A 1941 *J. Appl. Mech.* **8** A169
[11] Yaglom A M 1987 *Correlation Theory of Stationary and Related Random Functions* (New York: Springer)
[12] Roux S 1995 Rugosités de Fracture: Observations et spéculations *Proc. MECAMAT (Aussois 1995)*
[13] Matsushita M and Ouchi S 1989 *Physica* **38D** 246
[14] Hinrichsen E L, Hansen A and Roux S 1989 *Europhys. Lett.* **8** 1
[15] Frantziskonis G, Renaudin P and Breysse D 1995 Heterogeneous solids—Part I: analytical and numerical 1-D results on adverse boundary related phenomena *Preprint*
[16] Renaudin P, Breysse D and Frantziskonis G 1995 Heterogeneous solids—Part II: numerical 2-D results on boundary and other relevant phenomena *Preprint*
[17] Meisner M J 1995 *PhD Dissertation* University of Arizona
[18] Schroeder M 1991 *Fractals, Chaos, Power Laws: Minutes From an Infinite Paradise* (New York: Freeman)
[19] Charmet J C, Roux S and Guyon E (ed) 1990 *Disorder and Fracture* (New York: Plenum) ch 2
[20] Roux S and Hansen A 1989 *Europhys. Lett.* **8** 729
[21] Herrmann H J and Roux S (ed) 1990 *Statistical Models for the Fracture of Disordered Media* (New York: North-Holland) ch 4
[22] Meneveau C and Sreenivasan K R 1987 *Phys. Rev. Lett.* **59** 1424
[23] Shinozuka M and Deodatis G 1991 *Appl. Mech. Rev.* **44** 191